International Conference on Control, Automation and Systems 2008
Oct. 14-17, 2008 in COEX, Seoul, Korea

Simulation of Human locomotion Using A Musculoskeletal Model

Taesoo Kim and Sungho Jo

Department of Electrical Engineering and Computer Science, KAIST, Daejeon, Korea
(Tel : +82-42-869-3540; E-mail: {tsgates, shjo}@kaist.ac.kr)

Abstract: Human gaits in a sagittal plane are simulated throughout a musculoskeletal model with a simple feedback postural controller. Hill-type muscletendon models generate joint motions over each leg. Typical human gait data about joint torques and angles is used to estimate muscular activation signal profiles by a simple optimization technique. A simple feedback controller updates the activation profiles to achieve stable dynamical walking simulation through optimization with a genetic algorithm. Simulation study demonstrates the proposed approach achieves realistic human walking behavior with neurophysiologically plausible muscular activations.

Keywords: Human locomotion; Hill-type muscletendon model; muscular activation; gait simulation.

1. INTRODUCTION

Human locomotion is an interesting research topic due to the fact that it is a fundamental movement in human behavioral science. Especially, physics-based locomotion models with biomechanical or neurobiological characteristics have been challenged [1]. This study suggests a technique to implement human behaviors such as biped locomotion based on a musculoskeletal model. The strategy in this paper uses neither direct optimization of physical or neuro-anatomical model parameters nor a detailed cost function. Therefore, the number of searched parameters is few and computational burden is little. It becomes possible due to a pre-computational process using a Hill-type muscletendon model.

2. COMPUTATIONAL MODEL

2.1 Kinematic and kinetic data of a gait cycle

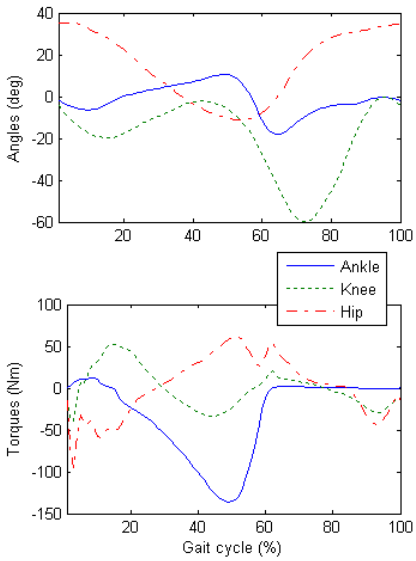

Fig.1.Typical joint angle and torque trajectories over a gait cycle. The angle convention is defined in Fig. 2.

Fig. 1 shows typical joint angle and torque trajectories of human gait cycle experimentally measured. The kinematic and kinetic information are used to compute the detailed muscular behaviors in the following sections.

2.2 Musculoskeletal model

Human body dynamics in the sagittal plane can be represented by a 7 segment, 6 d.o.f. linkage. Each leg consists of 3 segments, the thigh, the shank, and the foot, and segments are pivot-jointed. During gaits, each foot periodically interacts with the ground. The ground reaction is modeled as nonlinear spring-damper system without slipping. In case of slipping, dynamic frictional law is applied.

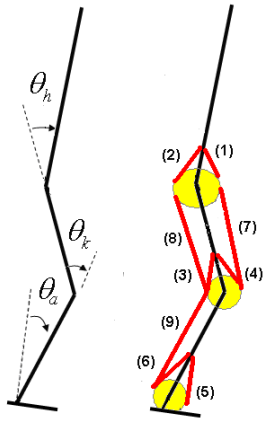

Fig.2. Joint and muscle configuration (only one leg shown for simplicity). The number is consistent with the muscle list in Table 1.

Body model incorporates nine representative muscles, six monoarticular and three biarticular muscles, attached around ankle, knee and hip joints (Fig. 2). Each muscle is modeled as serial connection of the contractile element(CE) and elastic element(SE) [2][3]. The CE muscle force is generated depending on the maximum isometric force ($F_{\max,i}$), force-velocity property, and

Table 1. Physical parameters in the muscletendon model

i	(1)	(2)	(3)	(4)	(5)	(6)	(7)	(8)	(9)
$F_{\max,i}$(N)	3000	2000	400	6000	1000	5000	1000	3000	1500
$l_{opt,i}$(m)	0.11	0.11	0.13	0.08	0.06	0.04	0.08	0.1	0.05
$l_{slack,i}$(m)	0.1	0.13	0.1	0.23	0.24	0.26	0.35	0.31	0.4
$\theta_{o,i}$(rad)	$\pi/6$	$\pi/6$	$\pi/9$	$\pi/3$	$5\pi/9$	$\pi/2$	$\pi/6$	$\pi/6$	$\pi/2$

muscular activation (a_i) [2][3].

$$F_{CE,i}(a_i,\dot{l}_{CE,i},l_{CE,i}) = a_i F_{\max,i} f_{v,i}(\dot{l}_{CE,i}) f_{l,i}(l_{CE,i})$$

for $i=1,...,9$ where $0 \le a_i \le 1$, $f_{l,i}(l_{CE,i})$ expresses the force-length property, and $f_{v,i}(\dot{l}_{CE,i})$ the force-velocity property.

The force-length property is expressed as [3][4].

$$f_{l,i}(l_{CE,i}) = \exp\left(c \left| \frac{l_{CE,i} - l_{opt,i}}{l_{opt,i} w} \right|^3 \right)$$

where l_{opt} is the optimum contractile element length for maximum force production. w determines the width of $f_l(l_{CE})$, and c is a coefficient (c =ln(0.05)).

The force-velocity property is characterized depending on whether the muscle shortens or lengthens [3][4].

$$f_{v,i}(\dot{l}_{CE,i}) = \begin{cases} \dfrac{v_{\max,i} - \dot{l}_{CE,i}}{v_{\max,i} + K\dot{l}_{CE,i}}, & \text{if } \dot{l}_{CE,i} < 0 \\ N + (N-1)\dfrac{v_{\max,i} + \dot{l}_{CE,i}}{7.56K\dot{l}_{CE,i} - v_{\max,i}}, & \text{if } \dot{l}_{CE,i} \ge 0 \end{cases}$$

where $v_{\max,i}$ is a maximum shortening velocity and set to $-12 l_{opt,i}$, N is the dimensionless value of $F_{CE,i}/F_{\max,i}$ with a lengthening velocity of $\dot{l}_{CE,i} = -v_{\max,i}$ ($N=1.5$ for computation), and K is a curvature constant and set to 5.

The SE muscle force is characterized by a nonlinear elastic force-length property [3][4].

$$F_{SE,i}(l_{SE,i}) = \begin{cases} F_{\max,i}\left(\dfrac{l_{SE,i} - l_{slack,i}}{\varepsilon l_{slack,i}} \right)^2, & \text{if } \varepsilon > 0 \\ 0, & \text{if } \varepsilon \le 0 \end{cases}$$

where $l_{slack,i}$ is the tendon slack length, and ε represents the relative strain of the SE at maximal isometric force.

Geometric relation between joint angles and muscletendon length drives

$$\bar{l}_{MTC} = \bar{l}_{SE} + \bar{l}_{CE} = \bar{l}_{slack} + \bar{l}_{opt} + f(\bar{\theta},\bar{\theta}_o)$$

where $\bar{\theta}_o$ is the reference angles at rest, $\bar{l}_{SE}$ the SE lengths, $\bar{l}_{CE}$ the CE lengths, and $f(\bar{\theta},\bar{\theta}_o)$ represents the relation between joint angles and muscle lengths as in Table 2.

The joint angle trajectories are provided from experiments as in section 2.1. Therefore, the SE length can be described by the CE length and joint angles.

$$\dot{l}_{CE,i} = f_{v,i}^{-1}\left(\frac{F_{CE,i}(a_i,\dot{l}_{CE,i},l_{CE,i})}{a_i F_{\max,i} f_{l,i}(l_{CE,i})} \right) = f_{v,i}^{-1}\left(\frac{F_{SE,i}(l_{SE,i})}{a_i F_{\max,i} f_{l,i}(l_{CE,i})} \right) = f_{v,i}^{-1}\left(\frac{\hat{F}_{SE,i}(l_{CE,i})}{a_i F_{\max,i} f_{l,i}(l_{CE,i})} \right)$$

$$l_{CE,i} = \int_{t_0}^{t} f_{v,i}^{-1}\left(\frac{\hat{F}_{SE,i}(l_{CE,i})}{a_i F_{\max,i} f_{l,i}(l_{CE,i})} \right) dt$$

The neuromuscular activation dynamics is described [3] as: $\dot{a}_i + \frac{1}{\tau_{act}}(\beta + (1-\beta)u_i)a_i = \frac{1}{\tau_{act}}u_i$

where $\delta \le a_i \le 1$, and τ_{act} is the activation time constant, and τ_{act}/β is the deactivation time constant. The activation dynamics provides the muscular activation a_i from the descending neural signal u_i. δ is a small value representing baseline activation.

The joint torques($\bar{\tau}$) and the muscle forces are related via the moment arm matrix ($M(\bar{\theta})$)based on biomechanical anatomy[1].

$$\bar{\tau} = M^T(\bar{\theta})\bar{F}_{CE}(\bar{a},\dot{\bar{l}}_{CE},\bar{l}_{CE}) = M^T(\bar{\theta})\bar{F}_{SE}(\bar{l}_{SE})$$

2.3 Activation estimation

From the above equation, the following optimization problem is driven: at each time t,

$$\bar{x}^*(t) = \arg\min_{\bar{x}(t)} \frac{1}{2}(\bar{\tau}(t) - A(t)\bar{x}(t))^T(\bar{\tau}(t) - A(t)\bar{x}(t)) + \gamma \bar{x}^T(t)\bar{x}(t)$$

subject to $0 \le x_i(t) \le \left(\dfrac{l_{MTC,i}(t) - l_{slack,i}}{\varepsilon l_{slack,i}} \right)^2$, as long as $l_{MTC,i}(t) > l_{slack,i}$, and $x_i(t) = 0$ otherwise, $\forall i = 1,...,9$,

where $\bar{x} = \left(\dfrac{\bar{l}_{SE} - \bar{l}_{slack}}{\varepsilon \bar{l}_{slack}} \right)^2$.

The regularization term $\gamma \bar{x}^T(t)\bar{x}(t)$ is added to minimize the value of $\bar{x}(t)$. This is the quadratic programming with bounded variables. Its solving algorithm is already developed [6]. Once after $\bar{x}^*(t)$ is found, e.g., the SE force is determined, the SE length is obtained from: $l_{SE,i}(t) = l_{slack,i} + \varepsilon l_{slack,i}\sqrt{x_i(t)}$.

Table 2. Muscletendon length

	Muscletendon length
(1)	$l_{MTC,1} = l_{slack,1} + l_{opt,1} - 0.08(\theta_h - \theta_{o,1})$
(2)	$l_{MTC,2} = l_{slack,2} + l_{opt,2} + 0.08(\theta_h - \theta_{o,2})$
(3)	$l_{MTC,3} = l_{slack,3} + l_{opt,3} + 0.06\cos(\theta_k - \theta_{o,3})$
(4)	$l_{MTC,4} = l_{slack,4} + l_{opt,4} - 0.06\cos(\theta_k - \theta_{o,4})$
(5)	$l_{MTC,5} = l_{slack,5} + l_{opt,5} + 0.03\cos(\theta_a + \theta_{o,5})$
(6)	$l_{MTC,6} = l_{slack,6} + l_{opt,6} - 0.06\cos(\theta_a + \theta_{o,6})$
(7)	$l_{MTC,7} = l_{slack,7} + l_{opt,7} - 0.08(\theta_h - \theta_{o,7}) + 0.06(1 - \cos\theta_k)$
(8)	$l_{MTC,8} = l_{slack,8} + l_{opt,8} + 0.08(\theta_h - \theta_{o,7}) - 0.06(1 - \cos\theta_k)$
(9)	$l_{MTC,9} = l_{slack,9} + l_{opt,9} - 0.06\cos(\theta_a - \theta_{o,9}) - 0.06(1 - \cos\theta_k)$

Then, the CE length can be decided as:

$$\bar{l}_{CE}(t) = \bar{l}_{slack} + \bar{l}_{opt} + f(\bar{\theta}(t), \bar{\theta}_o) - \bar{l}_{SE}(t)$$

The SE is comparatively much stiffer than the CE, therefore, it is assumed, for computational simplicity, that $\dot{\bar{l}}_{SE} \approx \bar{0}$. Hence, $\dot{\bar{l}}_{CE} = \nabla_{\bar{\theta}} f(\bar{\theta}, \bar{\theta}_o)\dot{\bar{\theta}}$.

Using the estimations of $F_{SE,i}$, $l_{CE,i}$, and $\dot{l}_{CE,i}$, the activation can be estimated by

$$a_i(t) = \frac{F_{SE,i}(t)}{F_{\max,i} f_{v,i}(\dot{l}_{CE,i}(t)) f_{l,i}(l_{CE,i}(t))}$$

2.4 Optimization using genetic algorithm (GA)

It is not expected that the feedforward command $\bar{a}$ alone can realize stable locomotion. Therefore, a simple feedback control of the trunk pitch angle is attached to help postural maintenance.

$$\bar{u}_d = diag\{\bar{s}\}\bar{a} + \left(k_p(\theta_{pitch\_des} - \theta_{pitch}) - b_p\dot{\theta}_{pitch}\right)$$

where θ_{pitch}, $\dot{\theta}_{pitch}$ are respectively trunk pitch angle and velocity, and k_p, b_p are control parameters, and $\bar{u}_d$ is the input to neuromuscular dynamics in Eq.(1).

The 9 elements in $\bar{s}$ are parameters to be determined by the genetic algorithm according to the following cost function to be minimized:

$$C = \lambda_1\left(x_{c,trunk}(t_f) - l_{dist}\right)^2 + \lambda_2\left(\exp(\alpha(y_{c,trunk} - y_o^u)) + \exp(-\alpha(y_{c,trunk} - y_o^d))\right)$$

where $(x_{c,trunk}, y_{c,trunk})$ is the COM position of the upper body, and l_{dist} is a expected walking distance in t_f seconds, y_o^u is a feasible upper limit of $y_{c,trunk}$, and y_o^d is a feasible lower limit of $y_{c,trunk}$. λ_1, λ_2 and α are constants.

3. RESULTS

Typical GA terminates optimization after trial-error tuning of some in 30 generations as seen in Fig. 3. The optimized value of $\bar{s}$ is :

$\bar{s} = [4 \quad 8 \quad 2.57 \quad 3 \quad 0.69 \quad 0.82 \quad 6.71 \quad 3.29 \quad 4.67]^T$.

The optimized values decide the muscular activation profiles as in Fig. 4. The activations are comparable with typical patterns from human nominal gaits as indicated in Fig. 4. Using the activation profiles and a simple feedback control of trunk pitch angle, the proposed model can achieve stable gaits. Without losing stability, human gaits are continuously implemented. Fig. 5. shows sequential motion clips over a steady gait.

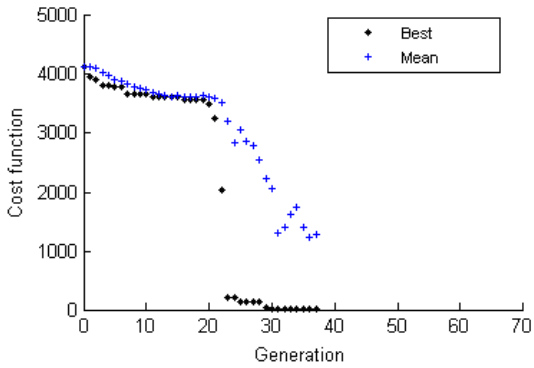

Fig. 3. The best and mean cost values over generation in GA.

4. CONCLUSIONS

Fig.6 illustrates the proposed musculoskeletal model interacting with the GA optimization. This study demonstrates the proposed scheme provides a way to compute neurophysiologically plausible muscular activation for modeling once information on joint torques and angles are provided. The approach may be used as a way of evaluating or helping modeling of a neural system.

The algorithm in Fig. 6 is applicable for any behavioral simulation with joint torque and angle information. Muscular activity in reality is very noisy and spiky. Therefore, even though detected, it is hard to imbed the muscular activity into computational models. Joint motions and torques are relatively easy to be measured or estimated. The approach predicts muscular activation indirectly.

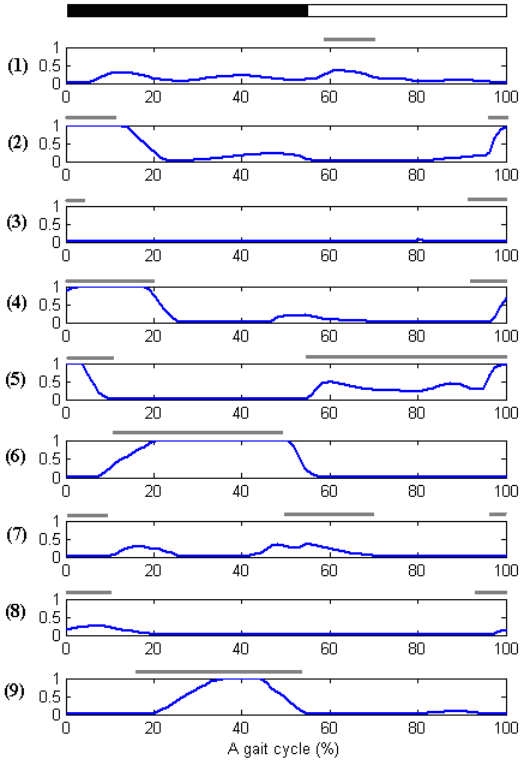

Fig.4. Averaged muscular activation patterns ($\bar{a}_d$) for simulation. A bar on the top indicates stance (back) and swing (while) phases. Numbers on the left side indicate corresponding muscles in Fig.1. Bars above each muscular activation pattern show typical electromyographic activities during human gait from literature [5].

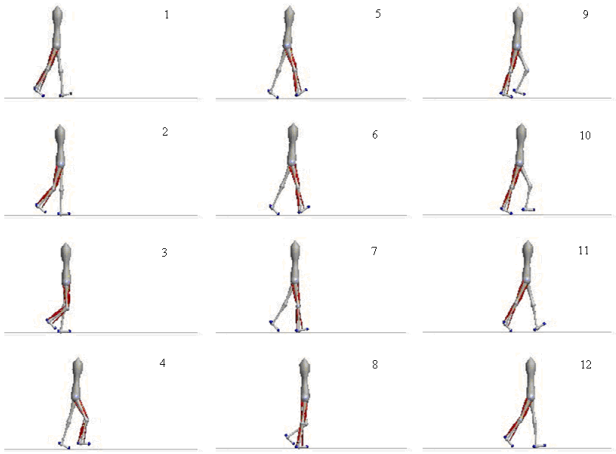

Fig. 5. Sequential clips for a steady gait cycle.

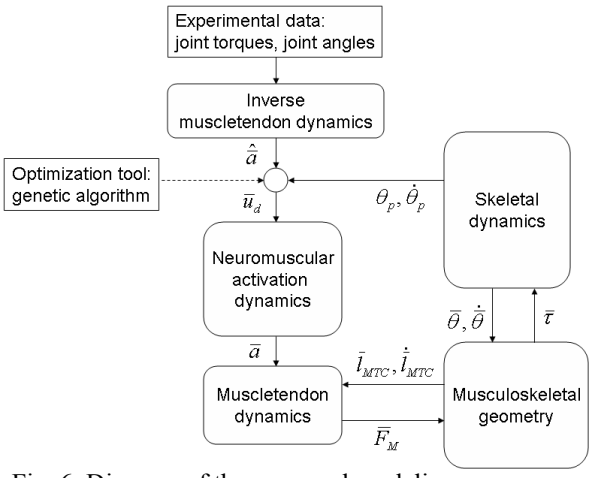

Fig. 6. Diagram of the proposed modeling

REFERENCES

[1] S. Jo, S. G. Massaquoi, A model of cerebrocerebello-spinomuscular interaction in the sagittal control of human walking, *Biol Cybern* 96(3) pp. 279-307.

[2] S. L. Delp, *Surgery simulation: a computer graphics system to analyze and design musculoskeletal reconstructions of the lower extremity*, PhD thesis, Stanford University, 1990.

[3] F. E. Zajac, Muscle and tendon: properties, models, scaling, and application to biomechanics and motor control, In: Bourne J(ed) CRC critical reviews in biomedical engineering, 17. CRC Press, Boca Raton: 359-411, 1989.

[4] A. J. Van Soest, M. F. Bobbert, The contribution of muscle properties in the control of explosive movements. *Biol Cybern* 69 pp. 195-204, 1993.

[5] J. Rose, J. G. Gamble JG, *Human walking*, 2nd ed., Williams & Wilkins, Baltimore, Maryland, USA, 1994.

[6] T. F. Coleman, Y. Li, A reflective Newton method for minimizing a quadratic function subject to bounds on some of the variables, *SIAM J Optimization* 6(4) pp. 1040-1058, 1996.